



ELSEVIER

Mechanics of Materials 32 (2000) 769–783

**MECHANICS
OF
MATERIALS**

www.elsevier.com/locate/mechmat

Modeling of interface cracks in fiber-reinforced composites with the presence of interphases using the boundary element method

Yijun J. Liu ^{*}, Nan Xu

Department of Mechanical Engineering, University of Cincinnati, P.O. Box 210072, Cincinnati, OH 45221-0072, USA

Received 2 August 1999; received in revised form 20 March 2000

Abstract

An advanced boundary element method (BEM) with thin-body capabilities was developed recently for the study of interphases in fiber-reinforced composite materials (Y.J. Liu, N. Xu and J.F. Luo, Modeling of interphases in fiber-reinforced composites under transverse loading using the boundary element method, ASME J. Appl. Mech. 67 (2000) 41–49). In this BEM approach, the interphases are modeled as thin elastic layers based on the elasticity theory, as opposed to spring-like models in the previous BEM and some FEM work. In the present paper, this advanced BEM is extended to study the interface cracks at the interphases in the fiber-reinforced composites. These interface cracks are curved cracks between the fiber and matrix, with the presence of the interphases. Stress intensity factors (SIFs) for these interface cracks are evaluated based on the developed models. The BEM approach is validated first using available analytical and other numerical results for curved cracks in a single material and straight interface cracks between two materials. Then, the interface cracks at the interphases of fiber-reinforced composites are studied and the effects of the interphases (such as the thickness and materials) on the SIFs are investigated. As a special case, results of the SIFs for sub-interface cracks are also presented. It is shown that the developed BEM is very accurate and efficient for the interface crack analyses, and that the properties of the interphases have significant influences on the SIFs for interface cracks in fiber-reinforced composites. © 2000 Elsevier Science Ltd. All rights reserved.

Keywords: Interface cracks; Interphases; Composites; Boundary element method

1. Introduction

Interphases in fiber-reinforced composite materials are thin layers of materials between the fiber and matrix, and play a very important role in the functionality and reliability of the composite materials (Chawla, 1998; Hyer, 1998). The effective utilization of the strength and stiffness of the fiber-

reinforced composites depends on efficient load transfers from the matrix to fibers through the interphases. However, during the manufacturing of composites, a large number of micro-cracks may develop, especially at the interfaces, even before any load has been applied. More interface cracks may develop during the loading process because of the differences in the stiffness of the fibers, interphases and matrix, resulting weak bonds at these interfaces. It is therefore essential to predict when an interface crack will become unstable

^{*} Corresponding author.

E-mail address: yijun.liu@uc.edu (Y.J. Liu).

in the fiber-reinforced composite materials, in order to provide some guidelines in improving the design of such materials.

Interface cracks between two dissimilar materials have been studied for at least four decades (Williams, 1959). Some of the analytical work and extensive reviews can be found, for example, in (Sinclair, 1980; Gautesen and Dundurs, 1987; Hutchinson et al., 1987; Rice, 1988; Suo and Hutchinson, 1990) for interface cracks between two isotropic materials, and in (Bassani and Qu, 1989; Qu and Bassani, 1989; Suo, 1990; Qu and Bassani, 1993) for interface cracks between two anisotropic materials. All of the above analytical work focus on straight interface cracks in 2D, infinitely large models of dissimilar materials. Curved interface cracks as existing between the fibers and matrix under transverse loading were studied recently in (Chao and Laws, 1997). Although the matrix is assumed to be infinitely large in this work, the analytical results have provided very important information about the stress singularities and contact zone sizes near the crack tip. For example, it is shown in (Chao and Laws, 1997) that the contact zones near the crack tip, where earlier analytical solutions have predicted overlapping of the crack faces and oscillatory singularity of the stresses, are indeed very small – only about 0.1% of the total crack length. All the analytical works mentioned above have provided the theoretical background and guidelines for numerical methods in the studies of interface cracks in materials or structures of more realistic geometries and under more complex loading conditions.

Numerical simulations using the finite element method (FEM) or the boundary element method (BEM) are effective methods for the study of crack problems. The boundary integral equation/boundary element method (BIE/BEM), pioneered in (Rizzo, 1967) for elasticity problems, has been demonstrated to be a viable alternative to the FEM for many problems in engineering, due to its features of boundary-only discretization and high accuracy (see, for example, Mukherjee, 1982; Cruse, 1988; Brebbia and Dominguez, 1989; Banerjee, 1994). The high accuracy and efficiency of the BEM for stress analysis, especially in fracture mechanics (Cruse, 1988; Cruse, 1996), is well

recognized because of its semi-analytical nature and boundary-only discretization. Analytical fundamental solutions (Green's functions) are employed as the engine in the BEM to generate, first numerical solutions on the boundary, then solutions anywhere inside the domain (if desired). The discretization errors in the BEM are mainly confined to the boundary of the structure and interfaces between different materials. The meshing for the BEM is also much more efficient than that for other domain-based methods, especially for problems with changing boundaries such as crack propagation problems.

The BIE/BEM has been applied to fracture mechanics analysis ever since its early days of development (Cruse, 1988; Cruse, 1996). The BEM can deal effectively with straight cracks, curved cracks (Zang and Gudmundson, 1988; Paulino et al., 1993), interface cracks in isotropic materials (Miyazaki et al., 1993; Xiao and Hui, 1994; Yuuki and Xu, 1994; Sladek and Sladek, 1995) or in anisotropic materials (Berger and Tewary, 1997), as well as wave scattering from cracks (Lin and Keer, 1987; Budreck and Achenbach, 1988; Krishnasamy et al., 1990; Krishnasamy et al., 1992; Liu and Rizzo, 1997). Other forms of the integral equation methods have also been applied to the interface crack analysis in the context of fiber-reinforced composites. In (Lee and Mal, 1997; Lee and Mal, 1998), the stress distributions near the interface cracks between the fiber and matrix were studied by a volume integral method. The interphases between the fiber and the matrix were considered in these models in which the matrix was assumed to extend to infinity. Interactions of a cluster of fibers were also investigated in (Lee and Mal, 1997; Lee and Mal, 1998). Another integral equation approach was developed recently in (Helsing, 1999) to study the interface crack of a general shape. An interesting example was presented, in which the stress intensity factors (SIFs) were computed for a crack at the interface of an inclusion (fiber) with 19 protruding arms and embedded in an infinite elastic plane (matrix).

However, no interface cracks between the fiber and matrix with the presence of the interphases have been studied by the BEM. This may be related to the fact that the BEM had been regarded

until recently as difficult, if not impossible, to deal with thin bodies such as the interphases. Recently, an advanced BEM with thin-body capabilities was developed for the studies of the interphases in fiber-reinforced materials (Liu et al., 2000), and coatings or thin films (Luo et al., 1998; Luo et al., 2000). In this BEM approach, the interphases are modeled as thin elastic layers using the elasticity theory, as opposed to the spring-like models in the previous BEM (Achenbach and Zhu, 1989; Achenbach and Zhu, 1990; Pan et al., 1998) and some FEM work. The developed BEM approach is found to be extremely accurate and efficient for the analysis of thin and layered structures. By employing much fewer boundary elements (less than 200) for a whole unit-cell model, the developed BEM can provide accurate stress results for which the FEM has to employ more than 3500 elements for only a quarter model of the same unit-cell as reported in (Wacker et al., 1998).

In this paper, this advanced BEM approach is extended to the study of interface cracks in the interphase regions in fiber-reinforced composites. These interface cracks are curved cracks between the fiber and matrix, with the presence of the interphases. Stress intensity factors for these interface cracks are calculated based on the developed models. The BEM approach is validated first using available analytical and other numerical results for curved cracks in a single material and straight interface cracks between two materials. Then, the interface cracks in the interphase regions of fiber-reinforced composites are studied and the effects of the interphases (such as the thickness and materials) on the SIFs are investigated. As a special case, results of the SIFs for sub-interface cracks are also presented. It is shown that the developed BEM is very efficient for the interface crack analyses and that the properties of the interphases have significant influences on the SIFs for interface cracks in fiber-reinforced composites.

2. BIE formulation

The following conventional BIE for two-dimensional, isotropic, linearly elastic structures

(Rizzo, 1967) is applied in this study (index notation is used here):

$$C_{ij}(P_0)u_j^{(\beta)}(P_0) = \int_S \left[U_{ij}^{(\beta)}(P, P_0)t_j^{(\beta)}(P) - T_{ij}^{(\beta)}(P, P_0)u_j^{(\beta)}(P) \right] dS(P) \quad (1)$$

in which $u_i^{(\beta)}$ and $t_i^{(\beta)}$ are the displacement and traction fields, respectively, $U_{ij}^{(\beta)}(P, P_0)$ and $T_{ij}^{(\beta)}(P, P_0)$ the displacement and traction kernels (Kelvin's solution or the fundamental solution), respectively, P the field point, (P_0) the source point, S the boundary of a single material domain V , $C_{ij}(P_0)$ a constant coefficient matrix depending on the smoothness of the curve S at the source point P_0 . The superscript β on the variables in Eq. (1) signifies the dependence of these variables on the material domain. The expressions for the kernel functions $U_{ij}^{(\beta)}(P, P_0)$ and $T_{ij}^{(\beta)}(P, P_0)$, which contain the material constants, can be found in (Liu et al., 2000) or any other references on the BEM (see, e.g., Mukherjee, 1982; Brebbia and Dominguez, 1989; Banerjee, 1994).

BIE (1) is applied to each material domain (matrix, fiber and interphase), which will relate the boundary displacement and traction fields in that domain only. The multi-domain method is employed, where each crack surface is modeled as part of the boundary of the domain. The resulting BIEs from each domain are coupled through the interface conditions. The continuity of the displacement and traction is imposed at the perfectly bonded interface, while traction-free condition is applied on the interface crack faces. The isoparametric quadratic boundary (line) elements are applied in this study. Details of coupling the BIEs from each domain and the numerical implementations can be found in (Luo et al., 1998; Liu et al., 2000).

There have been several questions or concerns in the BEM community about applying the conventional BIE (1) to crack problems and thin shell-like problems. Is the conventional BIE (1) suitable for analyzing such problems? If it is, how to deal with the nearly singular integrals arising from such problems when parts of the boundary are very close to each other? It is well known (Cruse, 1988) that the conventional BIE (1) will degenerate when

it is applied to bodies containing a crack which is modeled as two separate faces (curves in 2D or surfaces in 3D). The equation at a point on one face of the crack is identical to the equation at a point on the opposing face, if the crack opening is approaching zero. The corresponding two rows in the matrix for the linear algebra equations are the same and this leads to the degeneracy of the linear system (the matrix is singular). To solve this degeneracy difficulty in the BEM for crack problems, the hypersingular BIE, which is the derivative of the conventional BIE (1), is introduced and has been applied successfully in the BEM for crack problems (see, e.g., Gray et al., 1990; Krishnasamy et al., 1990; Liu and Rizzo, 1997). Another remedy to this degeneracy is to introduce artificial boundaries, starting from the crack tips and leading to the outer boundary, therefore dividing the original domain into two sub-domains. BIE (1) is applied in each sub-domain separately with the crack faces as boundaries for the sub-domains. The resulting two systems of equations from each domain are coupled together using the continuity (interface) conditions on the artificial boundaries. In this way the degeneracy can be avoided. For interface cracks sitting between two materials (sub-domains), BIE (1) must be applied to each material domain and the crack faces are treated as part of the boundary of the sub-domains. Therefore the degeneracy issue of the conventional BIE does not exist for analyzing interface crack problems using the BEM.

For thin shell-like structures or materials, such as the interphases in fiber-reinforced composite materials, it has been shown recently (Liu, 1998) that conventional BIE (1) will not degenerate, contrary to the case of a crack in one material for which BIE (1) does degenerate, as discussed above. The main obstacle in applying BIE (1) for thin shell-like structures is therefore the nearly-singular integrals existing in the BIE when integrations need to be done on one surface while the source point is on the other closely nearby surface. Efficient analytical and numerical procedures have been devised for computing such nearly-singular integrals for both 3D (Liu et al., 1993; Liu, 1998) and 2D (Luo et al., 1998) problems. Excellent numerical results have been obtained for various

thin shell-like structures using these advanced techniques in dealing with thin bodies or thin shell-like structures (Liu et al., 1993; Liu and Rizzo, 1997; Liu, 1998; Luo et al., 1998; Liu and Chen, 1999; Liu et al., 2000; Luo et al., 2000).

In the recent work in (Liu et al., 2000), interphases in unidirectional fiber-reinforced composites under transverse loading are modeled successfully by the BEM based on the elasticity theory. The interphases are regarded as elastic layers between the fiber and matrix, as opposed to the spring-like models in the BEM literature. Both cylinder and square unit-cell models of the fiber-interphase-matrix systems are considered. The effects of varying the modulus and thickness (including nonuniform thickness) of the interphases with different fiber volume fractions are investigated. Numerical results demonstrate that the developed BEM is very accurate and efficient in determining the interface stresses and effective elastic moduli of fiber-reinforced composites with the presence of interphases of arbitrarily small thickness and nonuniform thickness.

In this paper, the BIE as given in Eq. (1) and with the thin-body capabilities developed in (Luo et al., 1998; Liu et al., 2000) for 2D elastic thin structures are extended to study the stress distributions and stress intensity factors for fiber-reinforced composites containing interface cracks, with or without the presence of the interphases between the fiber and matrix.

3. Stress intensity factors (SIFs)

Formulas scattered in the literature for calculating the stress intensity factors for cracks in one material and interface cracks between two materials are listed in this section for convenience.

For a flat, homogeneous and isotropic plate with a center crack of length $2a$ (in the x -direction) and width $2w$, subjected to a uniform tension σ_0 (in the y -direction), the SIF K_1 is given by the following expression (see, e.g., (Hellan, 1984)):

$$K_1 = \sigma_0 \sqrt{\pi a} \left[\frac{1 - 0.5a/w + 0.326a^2/w^2}{\sqrt{1 - a/w}} \right]. \quad (2)$$

For an infinitely large plate ($w \rightarrow \infty$), this expression is reduced to the familiar result $K_1 = \sigma_0 \sqrt{\pi a}$.

For an interface crack with the length $2a$ and between two dissimilar materials subjected to a uniform tension σ_0 , an analytical expression for the stress intensity factors K_1 and K_2 is given in the following complex form (Rice, 1988):

$$K_1 + iK_2 = \sigma_0(1 + 2i\varepsilon)(2a)^{-ie} \sqrt{\pi a}, \quad (3)$$

where $i = \sqrt{-1}$, and

$$\varepsilon = \frac{1}{2\pi} \ln \left\{ \left(\frac{\kappa_1}{G_1} + \frac{1}{G_2} \right) / \left(\frac{\kappa_2}{G_2} + \frac{1}{G_1} \right) \right\}, \quad (4)$$

$$\kappa_\beta = 3 - 4\nu_\beta \quad (\text{for plane strain}),$$

$$\kappa_\beta = \frac{3 - \nu_\beta}{1 + \nu_\beta} \quad (\text{for plane stress})$$

with ν_β and G_β being the Poisson's ratio and shear modulus of the material β , respectively. In a different expression for $K_1 + iK_2$, given in (Yuuki and Xu, 1994), the constant multiplier $(2a)^{-ie}$ does not appear on the right-hand side of Eq. (3).

The stress intensity factors can be computed using the following two methods:

(1) *From crack opening displacements (the COD method)*. The following formulation is used to calculate the SIF from the crack opening displacement (Rice, 1988; Xiao and Hui, 1994):

$$K_1 + iK_2 = \frac{2(2\pi)^{1/2}(1 + 2i\varepsilon)[\cosh(\pi\varepsilon)](\Delta v + i\Delta u)}{Cr^{1/2+ie}}, \quad (5)$$

where $\Delta v + i\Delta u = (v + iu) |_{\theta=\pi} - (v + iu) |_{\theta=-\pi}$, u and v denote the displacements of the nodes behind the crack tip in the x - and y -directions, respectively, and (r, θ) is the polar coordinate with its origin at the (right) crack tip (distance r should be very small compared to the crack length $2a$). The material constant C is defined by

$$C = \frac{\kappa_1 + 1}{G_1} + \frac{\kappa_2 + 1}{G_2}. \quad (6)$$

(2) *From stresses ahead of the crack tip (the stress method)*. The relation of stresses ahead of the crack tip and the SIF for an interface crack can be expressed as (Rice, 1988):

$$K_1 + iK_2 = (\sigma_y + i\tau_{xy})r^{-ie} \sqrt{2\pi r}, \quad (7)$$

where σ_y and τ_{xy} are the tensile stress and shear stress, respectively, ahead of the crack tip, and r is the distance to the crack tip from the point where stresses are used in Eq. (7). To obtain more accurate results of K_1 and K_2 , only the points which are near the crack tip should be selected. From Eq. (7), it is easy to see that when $\varepsilon = 0$ and $(\tau_{xy}) = 0$, one obtains $K_1 = \sigma_y \sqrt{2\pi r}$, which is the result for one material case. Again, in a different expression given in (Yuuki and Xu, 1994), a constant multiplier $(2a)^{ie}$ appears on the right-hand side of Eq. (7).

4. Numerical examples

First, numerical examples are studied to verify the developed BEM approach to the analysis of interface cracks, using the available analytical and other numerical results for special cases in the literature. Then, the stress intensity factors for interface cracks in the fiber-reinforced composites are computed to demonstrate the efficiency and usefulness of the BEM for such applications. Quadratic line elements are used on the boundaries and interfaces of the material domains. In all the cases, the total number of boundary elements used are less than 200, which is in strong contrast to the FEM which requires a much large number of 2D finite elements even for the case without interface cracks (Wacker et al., 1998).

4.1. Straight cracks in a finite plate

4.1.1. Center crack in one material

To verify the developed BEM, the stress intensity factor for a center crack in a homogeneous plate (Fig. 1) is studied first. The quarter-point element (QPE) and double nodes (see, e.g., (Brebbia and Dominguez, 1989; Cook et al., 1989)) are used near the crack tip in the BEM model. Fig. 2 shows the BEM discretization around the crack tip (which is closed, not open as shown in Fig. 2). The plate is discretized using two regions (multi-domain approach, Fig. 1) and conventional

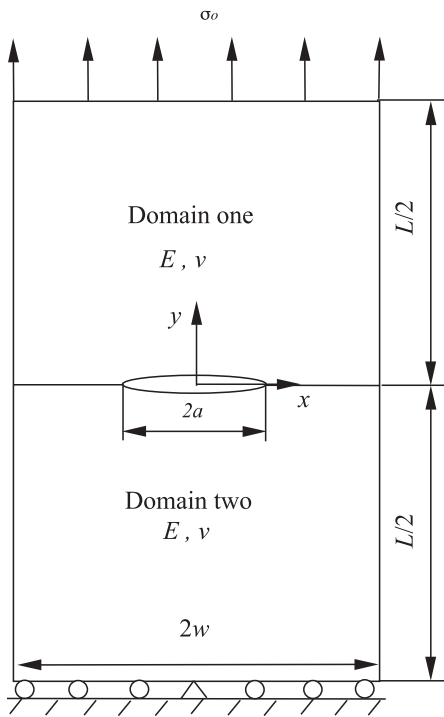


Fig. 1. A center crack in one homogeneous material.

BIE (1) is applied in each domain independently. In this multi-domain BEM approach to crack problems, the degeneracy issue of the conventional BIE is avoided (Cruse, 1988). The COD method and the stress method, discussed in Section 3, are applied in computing the SIF.

The following parameters are used for the calculation: $a = 1 \text{ mm}$, $w = 2.5 \text{ mm}$, $L = 10 \text{ mm}$, $\sigma_0 = 10^4 \text{ Pa}$.

Material properties are the same in domains one and two in this case, i.e., $E = 10^7 \text{ Pa}$ and $\nu = 0.3$.

Results of the normalized SIF $K_1^* = K_1 / (\sigma_0 \sqrt{\pi a})$ for this model is shown in Table 1. Compared with the theoretical value of SIF for an infinite plate (Eq. (2)), K_1^* obtained from the COD is found to be more accurate than that from the stresses. The result from stresses is more sensitive to the element type and size near the crack tip due to the singular behavior of the stresses near the crack tip. Smaller elements are needed in this region to obtain more accurate stress data.

Table 2 shows the normalized stress intensity factor of the center crack in one material with

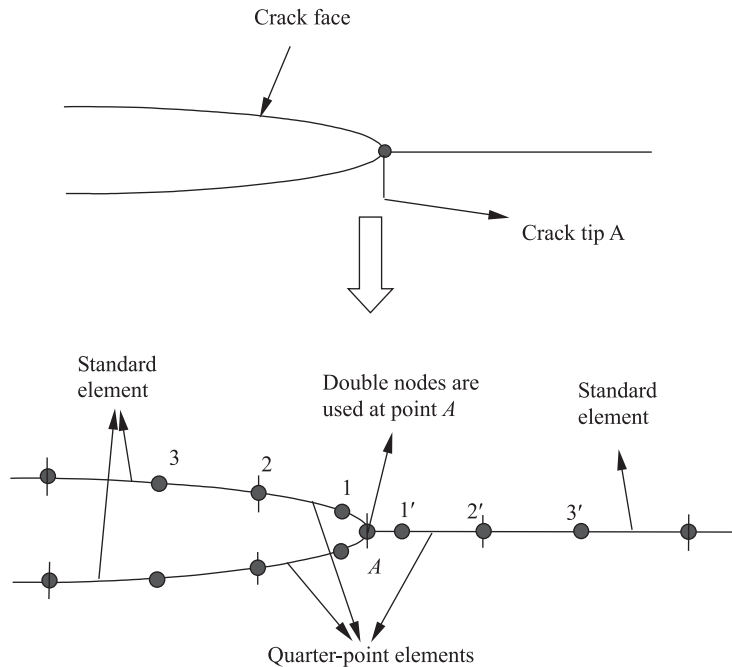


Fig. 2. Boundary element discretization around the crack tip.

Table 1
Normalized K_1 for a center crack in one material from the COD and stress^a

	Node location	Node 1 or 1'	Node 2 or 2'	Node 3 or 3'
COD	K_1^*	1.0294	1.0270	1.0126
	Error (%)	0.85	0.61	-0.80
Stress	K_1^*	1.1173	1.1881	1.2391
	Error (%)	9.45	16.39	21.38

^a Note: (1) $K_1^* = K_1/\sigma_0\sqrt{\pi a}$; The exact value is $K_1^* = 1.0208$; (2) Nodes 1, 2 and 3 are used in the COD method and 1', 2' and 3' in the stress method.

Table 2
Normalized K_1 for a center crack with different sizes in one material^a

	a/w	0.6	0.5	0.4	0.3	0.2	0.1	$a/w \rightarrow 0$
K_1^*	Present BEM	1.3025	1.1871	1.1067	1.0479	1.0131	0.9953	1.0000
	(Isida, 1973)	1.3033	1.1867	1.1094	1.0577	1.0246	1.0060	

^a Note: (1) $K_1^* = K_1/\sigma_0\sqrt{\pi a}$; (2) $K_1 = \sigma_0\sqrt{\pi a}$ as $a/w \rightarrow 0$.

different crack sizes (the ratio a/w varies from 0.1 to 0.6) by the COD method. Compared with the analytical results from Eq. (2), the maximum error in the BEM results is only 1.06%.

The good agreement of the SIF results using the COD in the above examples validates the developed BEM approach and demonstrates the accuracy of the COD method for calculating the SIF in this case. If not specified, all the SIF results for the following examples are computed based on the COD method.

4.1.2. Interface crack between two dissimilar materials

An interface crack in a bi-material plate subjected to uniform tension σ_0 ($= 10^4$ N) is considered, Fig. 3. The two materials used are Si_3N_4 and S45C with the following properties:

- Si_3N_4 : $E = 304$ GPa, $\nu = 0.27$;
- S45C : $E = 206$ GPa, $\nu = 0.30$.

Again, traction-free boundary conditions on the crack surfaces and the quarter-point element near the crack tips are used. The analysis was performed by changing the ratio of a/w from 0.1 to 0.6. Table 3 shows a comparison of the SIF results by the present BEM and those in (Yuuki and Xu, 1994) which is also based on a BEM approach. It is observed that the normalized stress intensity

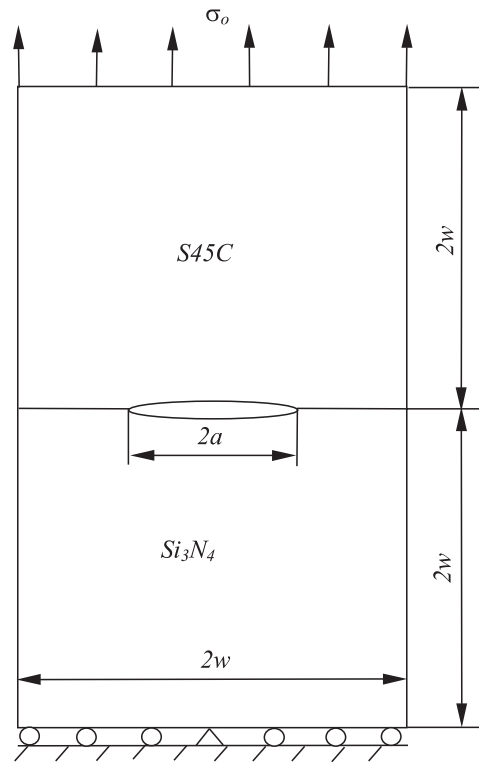


Fig. 3. Model of an interface crack under tension in a finite plate of dissimilar materials.

factor F_1 increases as the size of the crack increases, with the value oscillating around 1.0 (the theoretical value for an infinite plate with a center

Table 3
Normalized stress intensity factors for a center interface crack^a

a/w	K_1^*		K_2/K_1	
	Present BEM	Yuuki and Xu (1994)	Present BEM	Yuuki and Xu (1994)
0.6	1.3148	1.301	-0.0212	-0.012
0.5	1.1854	1.169	-0.0220	-0.015
0.4	1.0999	1.083	-0.0200	-0.010
0.3	1.0442	1.038	-0.0228	-0.020
0.2	1.0111	1.003	-0.0239	-0.022
0.1	0.9912	0.979	-0.0272	-0.026
0.0	1.000		-0.026	

^a Note: (1) $K_1^* = K_1/\sigma_0\sqrt{\pi a}$; (2) Values at $a/w = 0.0$ are the analytical solutions (Yuuki and Xu, 1994) for an interface crack in an infinite plate of dissimilar materials.

crack). The value of K_2/K_1 does not change monotonically as a/w increases. It should be pointed out that the bi-material constant ε given in (Yuuki and Xu, 1994) is -0.0113 , but the value from Eq. (7) for ε is -0.01285 in plane strain case which is the case assumed in (Yuuki and Xu, 1994). However, in order to compare with the results in (Yuuki and Xu, 1994), the first value for ε is used here. From Table 3, one can conclude that the present BEM approach can provide accurate SIFs for the interface crack problem studied.

4.2. Curved cracks in one material

A finite plate with a circular-arc crack loaded by uniform tension σ_0 in both x - and y -directions is shown in Fig. 4. The analytical solutions of the SIF for a circular-arc crack in an infinite plate under uniform bi-directional loading are available in (Sih, 1973). In the present numerical test, w/R is fixed at 5 and the half-crack angle α varies from 15° to 90° . Again, the traction-free boundary condition and the quarter-point elements are used. In Tables 4 and 5, the calculated stress intensity factors K_1 and K_2 , respectively, normalized with respect to $\sigma_0\sqrt{\pi R\alpha}$, are compared to the exact values for an infinite plate. It is observed that the maximum differences for K_1 and K_2 are only 1.32% and 3.06%, respectively. This excellent comparison is another strong indication that the present BEM approach can provide accurate SIF data for both straight and curved cracks.

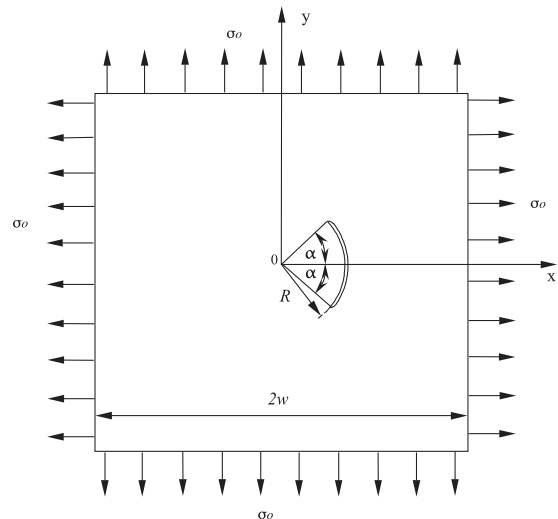


Fig. 4. A square plate under tension with a circular-arc crack (two domains with the same material are used – a circular and a square domains).

4.3. Curved interface cracks between the fiber and matrix

A square unit-cell model of a composite, shown in Fig. 5, with a circular-arc crack at the interface of the fiber and matrix (without the presence of the interphase), is studied. The applied boundary conditions are shown in Fig. 5, in which δ a given displacement. The fiber radius R is determined by the fiber volume fraction and the length $2w$ is equal to one in this unit-cell model. The half-crack angle α changes from 15° to 90° for the interface crack.

Table 4
Normalized K_1 for the circular–arc crack in one material^a

Angle α (°)	K_1^*		Errors (%)
	Present BEM	Sih (1973)	
15	0.962145	0.969272	0.7345
25	0.922027	0.917834	0.4568
30	0.896306	0.884647	1.3178
45	0.762705	0.764644	–0.2535
60	0.632476	0.630045	0.3859
75	0.498917	0.497235	0.3390
90	0.372517	0.376126	–0.9596

^a Note: $K_1^* = K_1/\sigma_0\sqrt{\pi R\alpha}$ (α is in radians for this factor).

Table 5
Normalized K_2 for the circular–arc crack in one material^a

Angle α (°)	K_2^*		Errors (%)
	Present BEM	Sih (1973)	
15	0.127215	0.127607	–0.3072
25	0.209626	0.203479	3.0209
30	0.236693	0.237041	–0.1468
45	0.31940	0.316726	–0.8443
60	0.369960	0.363757	1.7052
75	0.390917	0.381542	2.4571
90	0.387646	0.376126	3.0628

^a Note: $K_2^* = K_2/\sigma_0\sqrt{\pi R\alpha}$.

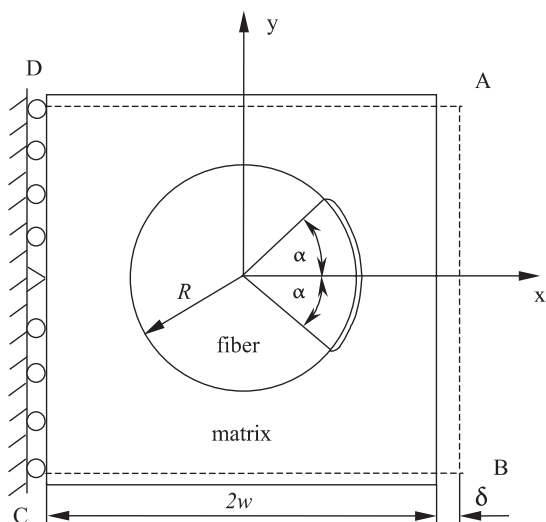


Fig. 5. A circular–arc interface crack between the fiber and matrix.

The properties of the constituent materials considered are:

for fiber : $E^{(f)} = 72.4 \text{ GPa } (10.5 \times 10^6 \text{ psi}),$

$\nu^{(f)} = 0.22;$

for matrix : $E^{(m)} = 3.45 \text{ GPa } (0.5 \times 10^6 \text{ psi}),$

$\nu^{(m)} = 0.35.$

The normalized stress intensity factors obtained using the present BEM are shown in Table 6. Three fiber volume fractions are considered. From Table 6, one can conclude that for a fixed volume fraction ratio, the maximum value of K_1 is corresponding to the minimum angle α , while the maximum value of K_2 occurs when α reaches the maximum. When $\alpha < 45^\circ$, K_1 decreases as the fiber volume ratio increases and this trend is reversed when $\alpha > 45^\circ$.

Table 6

Normalized stress intensity factors for the circular–arc interface crack in the composite with different fiber volume fractions^a

Angle α (°)	Fiber volume fractions (%)					
	20		40		60	
	K_1^*	K_2^*	K_1^*	K_2^*	K_1^*	K_2^*
15	1.3925	0.0644	1.1836	0.1095	1.0574	0.1140
25	1.3056	0.3573	1.1716	0.2714	1.0308	0.0911
30	1.2613	0.4403	1.1337	0.3304	1.0182	0.1637
45	0.9669	0.7233	0.9592	0.6123	1.0009	0.5018
60	0.7033	0.8899	0.7948	0.8714	0.9745	0.9079
75	0.3839	0.9794	0.4952	1.0732	0.7384	1.3035
90	0.0355	0.9226	0.1047	1.0832	0.3242	1.4727

^a Note: $K_1^* = K_1/\sigma_{\text{ave}}\sqrt{\pi R\alpha}$, $K_2^* = K_2/\sigma_{\text{ave}}\sqrt{\pi R\alpha}$, where σ_{ave} is the average normal stress on edge AB (see Fig. 5).

4.4. Curved interface cracks between the interphase and matrix

Finally, the most interesting and challenging case that an interface circular–arc crack existing in the fiber-reinforced composite with the presence of the interphase, as shown in Fig. 6, is studied. Because of the presence and thinness of the interphase, which can cause difficulties for both FEM and earlier BEM approaches, no previous numerical as well as analytical results have been reported in the literature. The model used for this case is the same one as used in the previous example (Fig. 5), except that an interphase is introduced.

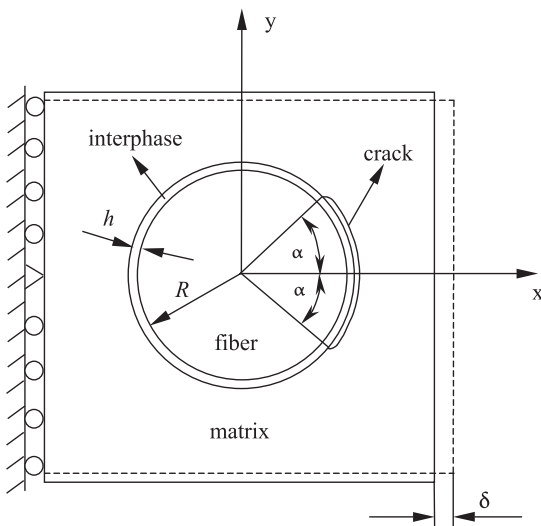


Fig. 6. A circular–arc crack between the interphase and the matrix.

The effects of the interphase thickness are studied first. The material properties used for the interphase are:

$$E^{(i)} = 36.2 \text{ GPa} (5.25 \times 10^6 \text{ psi}), \quad \nu^{(i)} = 0.30,$$

where the Young's modulus of the interphase has been taken as half of that of the fiber. The fiber volume fraction considered for this case is 60%, and the interphase thickness h varies from $h = 0.01R$ to $h = 0.05R$. The BEM mesh for $h = 0.05R$ is shown in Fig. 7, in which increased mesh density is employed at the two crack tips and uniform, larger mesh size is used elsewhere.

The normalized SIF K_1 and K_2 (with respect to $\sigma_{\text{ave}}\sqrt{\pi R\alpha}$, where σ_{ave} is the averaged tensile stress on the right edge, Fig. 6) for different interphase thickness are shown in Figs. 8 and 9, respectively, with the half-crack angle α changing from 15° to 90° . For comparison, the results for the previous case without the interphase, from the last two columns of Table 6, are also plotted in Figs. 8 and 9, respectively. It can be seen that for all the interphase thickness, in general, K_1 decreases and K_2 increases, as the angle α increases. For $\alpha < 45^\circ$, the effect of the interphase thickness on K_1 is not significant. For $\alpha > 45^\circ$, K_1 increases as the thickness of the interphase increases. The change of K_2 versus the interphase thickness is negligible until the angle α is in the range of 60° – 90° , where K_2 is larger for a thicker interphase.

The effects of the interphase materials are studied next. In this study, the material of the interphase is changing from that of the matrix to that of the fiber (see Section 4.3 for fiber and

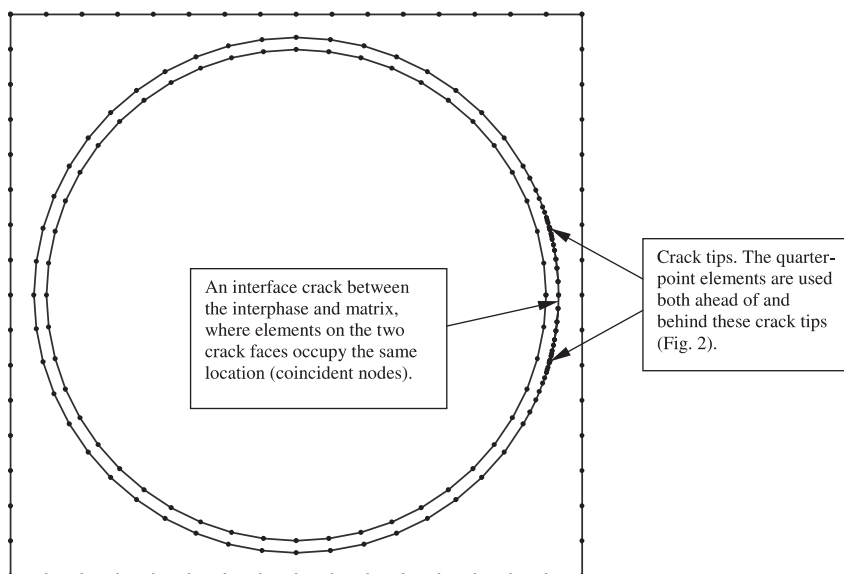


Fig. 7. The BEM mesh using quadratic line elements (three nodes form one element) for the unit-cell model with the circular-arc interface crack between the interphase and matrix (half-crack angle $\alpha = 15^\circ$, interphase thickness $h = 0.05R$, fiber volume fraction = 60%).

matrix material properties used), with five cases altogether (from material one to material five). For materials 2, 3 and 4, values of the Young’s modulus are 20.7 GPa (3.0×10^6 psi), 36.2 GPa (5.25×10^6 psi), and 58.6 GPa (8.5×10^6 psi), respec-

tively, and the Poisson’s ratio is fixed at 0.30. The fiber volume fraction is 60% for all the cases and the interphase thickness $h = 0.01R$. Figs. 10 and 11 show the BEM results of the normalized stress intensity factors K_1 and K_2 , respectively, for the

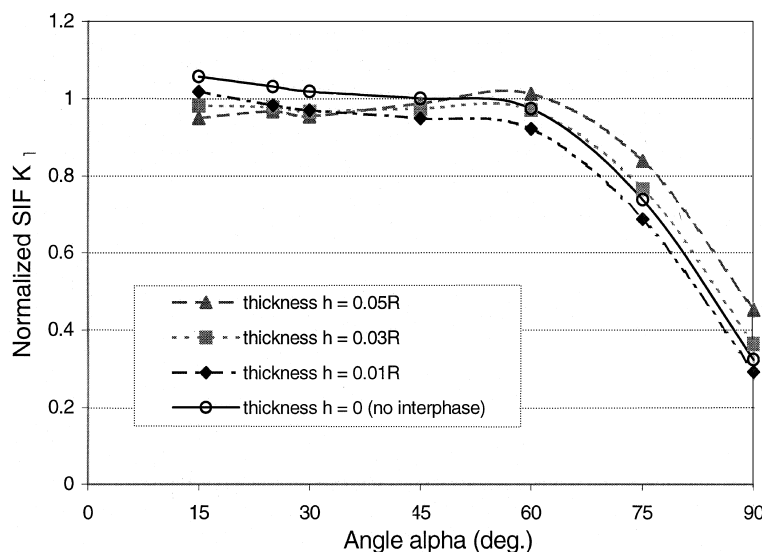


Fig. 8. Effects of the interphase thickness on the normalized stress intensity factor ($K_1/\sigma_{ave}\sqrt{\pi R\alpha}$) for the circular-arc interface crack.

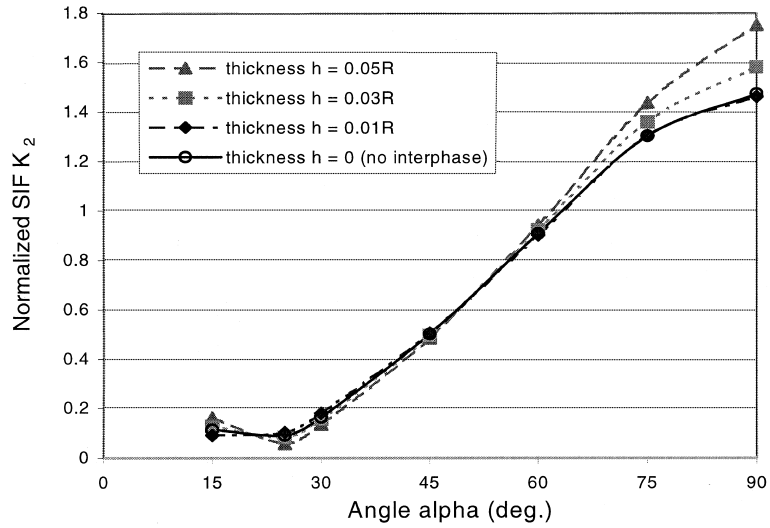


Fig. 9. Effects of the interphase thickness on the normalized stress intensity factor ($K_2/\sigma_{ave}\sqrt{\pi R\alpha}$) for the circular–arc interface crack.

circular–arc interface crack between the interphase and the matrix (Fig. 6). For comparison, the results of K_1 and K_2 for the case without the interphase (from the last two columns of Table 6) are also plotted in Figs. 10 and 11, respectively. In Fig. 10, it is observed that K_1 is much smaller when the interphase material is the same as the matrix (material 1). In this special case, the crack is ac-

tually a curved sub-interface crack in the matrix material and parallel to the interface of the fiber and the matrix with a distance of $0.01R$. This is in itself another class of interface crack problem (Hutchinson et al., 1987), which deserves further study. On the other hand, when the interphase material is the same as the fiber (material 5), K_1 values are very close to those for the case without

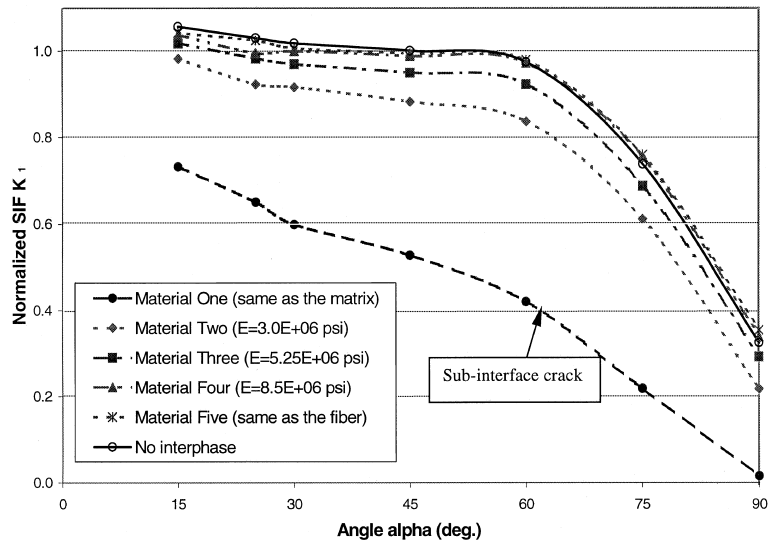


Fig. 10. Effects of the interphase materials on the normalized stress intensity factor ($K_1/\sigma_{ave}\sqrt{\pi R\alpha}$) for the circular–arc interface crack.

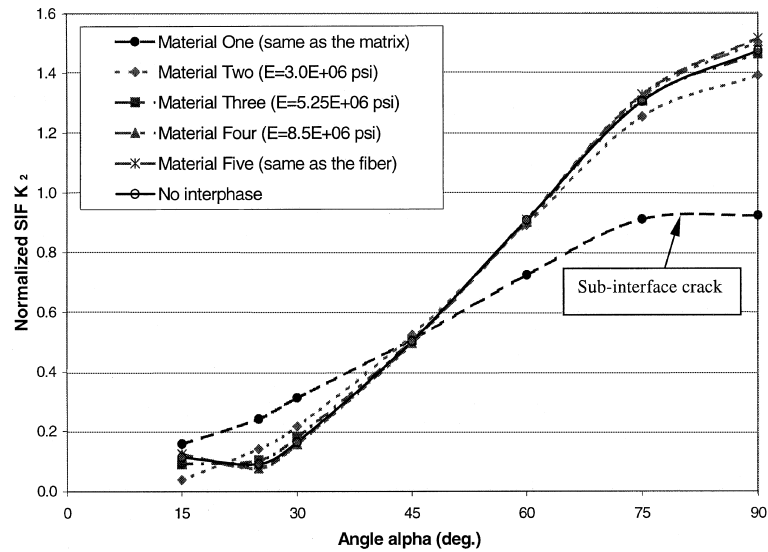


Fig. 11. Effects of the interphase materials on the normalized stress intensity factor ($K_2/\sigma_{ave}\sqrt{\pi R\alpha}$) for the circular-arc interface crack.

the interphase. Actually, this case is almost identical to the case without the interphase, except that the fiber radius is increased from R to $1.01R$. Results of K_2 (Fig. 11) show similar phenomenon, with the sub-interface crack results (material one) deviating substantially from the other interface crack results.

It should be pointed out that *no overlapping* of the two crack faces near the crack tips was observed in all the numerical studies presented above. This overlapping or contact of the crack faces is due to the oscillatory behavior of the displacement fields near the crack tips, predicted by the theory for linear, elastic interface crack problems (see, e.g., Rice, 1988; Chao and Laws, 1997). However, this oscillatory zone is extremely small as compared with the crack length. For example, the ratio of the length of this oscillatory zone to the crack length is only about 0.1% or smaller for a curved interface crack (Chao and Laws, 1997) and is less than 10^{-5} for a straight interface crack (Yuuki and Xu, 1994). In the current study, the size of the smallest elements employed near the crack tips is about 1% of the crack length, which is not small enough to capture the extremely small oscillatory zone predicted in the theory. The same observation was made

in (Yuuki and Xu, 1994) for the analysis of straight interface cracks using the BEM. Extremely fine mesh (with elements several orders smaller near the crack tips) would be needed to capture this overlapping zone, which may not improve the accuracy of the SIF calculation significantly. The quarter-point elements employed in the current study at the crack tips (Figs. 2 and 7) are intended to capture the dominating, singular behaviors of the stress fields near the crack tips, which exhibit the $1/\sqrt{r}$ singularity. Applications of such quarter-point elements near the crack tips have been proven very accurate and efficient in evaluating the stress intensity factors with reasonably fine mesh near the crack tips.

5. Conclusion

An advanced boundary element method has been developed to study the interface cracks in the fiber-reinforced composite materials with the presence of the interphases. Curved interface cracks have been studied and the results carefully verified using available analytical and other numerical results. Influences of the interphase thickness and material properties on the stress intensity

factors for the interface cracks, including the special case of sub-interface cracks, have been investigated. The numerical results demonstrate that the developed BEM is very accurate and efficient for the interface crack analysis for thin-layered structures, such as the interphases in composite materials. Extensions of the BEM to consider the thermal loading, multi-layered materials (coatings and thin films), contact models near the crack tip and 3D interface cracks will be interesting topics and can be carried out readily.

Acknowledgements

The support for this research by the National Science Foundation under the grant CMS 9734949 is gratefully acknowledged. The authors would like to thank the two reviewers for their suggestions to the manuscript.

References

- Achenbach, J.D., Zhu, H., 1989. Effect of interfacial zone on mechanical behavior and failure of fiber-reinforced composites. *J. Mech. Phys. Solids* 37 (3), 381–393.
- Achenbach, J.D., Zhu, H., 1990. Effect of interphases on micro and macromechanical behavior of hexagonal-array fiber composites. *J. Appl. Mech.* 57, 956–963.
- Banerjee, P.K., 1994. *The Boundary Element Methods in Engineering*. McGraw-Hill, New York.
- Bassani, J.L., Qu, J., 1989. Finite crack on bimaterial and bicrystal interfaces. *J. Mech. Phys. Solids* 37, 435–454.
- Berger, J.R., Tewary, V.K., 1997. Boundary integral equation formulation for interface cracks in anisotropic materials. *Comput. Mech.* 20, 261–266.
- Brebbia, C.A., Dominguez, J., 1989. *Boundary Elements – An Introductory Course*. McGraw-Hill, New York.
- Budreck, D.E., Achenbach, J.D., 1988. Scattering from three-dimensional planar cracks by the boundary integral equation method. *J. Appl. Mech.* 55, 405–412.
- Chao, R., Laws, N., 1997. The fiber–matrix interface crack. *J. Appl. Mech.* 64, 992–999.
- Chawla, K.K., 1998. *Composite Materials Science and Engineering*. Springer, New York.
- Cook, R.D., Malkus, D.S., Plesha, M.E., 1989. *Concepts and Applications of Finite Element Analysis*. Wiley, New York.
- Cruse, T.A., 1988. *Boundary Element Analysis in Computational Fracture Mechanics*. Dordrecht. Kluwer Academic Publishers, Netherlands.
- Cruse, T.A., 1996. BIE fracture mechanics analysis 25 years of developments. *Comput. Mech.* 18, 1–11.
- Gautesen, A.K., Dundurs, J., 1987. The interface crack in a tension field. *J. Appl. Mech.* 54, 93–98.
- Gray, L.J., Martha, L.F., Ingrassia, A.R., 1990. Hypersingular integrals in boundary element fracture analysis. *Int. J. Numer. Methods Engrg.* 29, 1135–1158.
- Hellan, K., 1984. *Introduction to Fracture Mechanics*. McGraw-Hill, New York.
- Helsing, J., 1999. On the numerical evaluation of stress intensity factors for an interface crack of a general shape. *Int. J. Numer. Methods Engrg.* 44, 729–741.
- Hutchinson, J.W., Mear, M.E., Rice, J.R., 1987. Crack paralleling an interface between dissimilar materials. *J. Appl. Mech.* 54, 828–832.
- Hyer, M.W., 1998. *Stress Analysis of Fiber-Reinforced Composite Materials*. McGraw-Hill, Boston.
- Isida, M., 1973. Analysis of stress intensity factor for the tension of a centrally cracked strip with stiffened edges. *Eng. Fract. Mech.* 5, 647.
- Krishnasamy, G., Rizzo, F.J., Liu, Y.J., 1992. Some advances in boundary integral methods for wave-scattering from cracks. *Acta Mechanica* 3 (Suppl), 55–65.
- Krishnasamy, G., Rudolph, T.J., Schmerr, L.W., Rizzo, F.J., 1990. Hypersingular boundary integral equations, some applications in acoustic and elastic wave scattering. *J. Appl. Mech.* 57, 404–414.
- Lee, J., Mal, A., 1997. A volume integral equation technique for multiple inclusion and crack interaction problems. *J. Appl. Mech.* 64, 23–31.
- Lee, J., Mal, A., 1998. Characterization of matrix damage in metal matrix composites under transverse loads. *Comput. Mech.* 21, 339–346.
- Lin, W., Keer, L.M., 1987. Scattering by a planar three-dimensional crack. *J. Acoust. Soc. Am.* 82, 1442–1448.
- Liu, Y.J., 1998. Analysis of shell-like structures by the boundary element method based on 3-D elasticity, formulation and verification. *Int. J. Numer. Methods Engrg.* 41, 541–558.
- Liu, Y.J., Chen, S.H., 1999. A new form of the hypersingular boundary integral equation for 3-D acoustics and its implementation with C^0 boundary elements. *Comput. Methods Appl. Mech. Engrg.* 173 (3–4), 375–386.
- Liu, Y.J., Rizzo, F.J., 1997. Scattering of elastic waves from thin shapes in three dimensions using the composite boundary integral equation formulation. *J. Acoust. Soc. Am.*, 102 (2), 926–932 (Pt.1, August).
- Liu, Y.J., Xu, N., Luo, J.F., 2000. Modeling of interphases in fiber-reinforced composites under transverse loading using the boundary element method. *ASME J. Appl. Mech.* 67, 41–49.
- Liu, Y.J., Zhang, D., Rizzo, F.J., 1993. Nearly singular and hypersingular integrals in the boundary element method. In: Brebbia, C.A., Rencis, J.J. (Eds.), *Boundary Elements XV. Computational Mechanics Publications*, Worcester, MA, pp. 453–468.

- Luo, J.F., Liu, Y.J., Berger, E.J., 1998. Analysis of two-dimensional thin structures from micro-to nano-scales using the boundary element method. *Comput. Mech.* 22, 404–412.
- Luo, J.F., Liu, Y.J., Berger, E.J., 2000. Interfacial stress analysis for multi-coating systems using an advanced boundary element method. *Comput. Mech.* 24 (6), 448–455.
- Miyazaki, N., Ikeda, T., Soda, T., Munakata, T., 1993. Stress intensity factor analysis of interface crack using boundary element method – application of contour-integral method. *Eng. Fract. Mech.* 45 (5), 599–610.
- Mukherjee, S., 1982. *Boundary Element Methods in Creep and Fracture*. Applied Science Publishers, New York.
- Pan, L., Adams, D.O., Rizzo, F.J., 1998. Boundary element analysis for composite materials and a library of Green's functions. *Comput. Struct.* 66 (5), 685–693.
- Paulino, G.H., Saif, M.T.A., Mukherjee, S., 1993. A finite elastic body with a curved crack loaded in anti-plane shear. *Int. J. Solids Struct.* 30 (8), 1015–1037.
- Qu, J., Bassani, J.L., 1989. Cracks on bimaterial and bicrystal interfaces. *J. Mech. Phys. Solids* 37, 417–433.
- Qu, J., Bassani, J.L., 1993. Interfacial fracture mechanics for anisotropic bimaterials. *J. Appl. Mech.* 60, 422–431.
- Rice, J.R., 1988. Elastic fracture mechanics concepts for interfacial cracks. *J. Appl. Mech.* 55, 98–103.
- Rizzo, F.J., 1967. An integral equation approach to boundary value problems of classical elastostatics. *Quart. Appl. Math.* 25, 83–95.
- Sih, G.C., 1973. *Handbook of Stress Intensity Factors*. Lehigh University, Bethlehem, PA.
- Sinclair, G.B., 1980. On the stress singularity at an interface crack. *Int. J. Fract.* 16 (2), 111–119.
- Sladek, J., Sladek, V., 1995. Boundary element analysis for an interface crack between dissimilar elastoplastic materials. *Comput. Mech.* 16, 396–405.
- Suo, Z., 1990. Singularities, interfaces and cracks in dissimilar anisotropic media. *Proc. R. Soc. London* 427 (A), 331–358.
- Suo, Z., Hutchinson, J.W., 1990. Interface crack between two elastic layers. *Int. J. Fract.* 43, 1–18.
- Wacker, G., Bledzki, A.K., Chate, A., 1998. Effect of interphase on the transverse Young's modulus of glass/epoxy composites. *Composites Part A* 29A, 619–626.
- Williams, M.L., 1959. The stresses around a fault or crack in dissimilar media. *Bull. Seismol. Soc. Am.* 49, 199–204.
- Xiao, F., Hui, C.-Y., 1994. A boundary element method for calculating the K field for cracks along a bimaterial interface. *Comput. Mech.* 15, 58–78.
- Yuuki, R., Xu, J.-Q., 1994. Boundary element method and its applications to the analyses of dissimilar materials and interface cracks. In: Nisitani, H. (Ed.), *Computational and Experimental Fracture Mechanics: Developments in Japan*. Computational Mechanics Publications, Southampton, UK, pp. 61–90.
- Zang, W., Gudmundson, P., 1988. A boundary integral method for internal piece-wise smooth crack problems. *Int. J. Fract.* 38, 275–294.